BEAM EMITTANCE DETERMINATION USING OPTICAL TRANSITION RADIATION

R.Chehab   M.Taurigna

G.Bienvenu

Laboratoire de l'Accélérateur linéaire, IN2P3 et Université de Paris Sud

F 91405 ORSAY Cedex

Abstract

Optical transition radiation produced by an electron beam, with an energy scaling from 80 keV to 20 MeV, on aluminium and silver foils, has been observed in backward direction. Count rates of photons were measured for three orders of magnitude of the electron energy. Emittance has been determined at 4.8 MeV, by the three gradient method, varying the spot size on Al foil with a solenoidal lens. Images of beam spots were observed on a sensitive CCD camera. A dedicated program on a PC computer allowed achievement of equidensity domains, X-Y profiles. Accurate determination of beam width provided emittance values which compared with those obtained with the traditional moving slit method present reasonable agreement.

1 INTRODUCTION

Investigation and monitoring of electron beam qualities require a precise determination of its emittance very often calculated by the three position or three gradient method. In such a case only beam dimensions have to be accurately measured. Therefore characteristics as sensitivity, resolution, dynamic range, rapidity are strongly dependent on the chosen profile monitor. We have studied at LAL-ORSAY a monitor based on the observation of the optical transition radiation (OTR) emitted by an electron beam crossing metallic foils at oblique incidence. Observation of the backward radiation was provided at different beam energies scaling from 80 keV to 20 MeV. Particular emphasis is put on emittance determination realized by the association of such monitor with a magnetic lens allowing beam dimensions variation.

2 THE TRANSITION RADIATION : A SHORT RECALL

Since the theoretical prediction of Ginzburg and Franck[1], the transition radiation gave rise to many experimental works; application to beam diagnostics presented an increasing interest since almost twenty years after the pioneer work of L.Wartski et al.[2] The relative sensitivity, of OTR, 10^{-2} photon per incident electron in the optical domain for particles in the range ($\gamma = 1 - 10^3$) makes this method easily practicable [3]. The absence of energy threshold as well as its simplicity make it also attractive for low energy beams [4].

The optical image of the electron beam is usually taken with a large acceptance angle of the optics. Therefore the yield integrated on angles much higher than the classical

emission angle γ^{-1}, and in the frequency interval (ω_1, ω_2) gives [3]:

$$N = \frac{\alpha}{\pi}[Ln(\gamma\theta)^2 - 1]Ln\frac{\omega_2}{\omega_1} \qquad (1)$$

where α is the fine structure constant ($\alpha = 1/137$)

Simulations concerning low energy beams - from some tens of keV to some MeV - based on theoretical work of Ashley [5]and experimental results of Mahan and Gallagher [6] have been worked out [7], They allowed useful estimation for the yield and helped the monitor design.

3 THE EXPERIMENTAL SET-UP

3.1 LAL Accelerator Test Facility (NEPAL)

The facility consists of a short linac ($E \leq 20\ MeV$) with a thermoionic gun; a bunching system made of prebuncher and buncher precedes a short accelerating section. Optics are provided with solenoidal lenses between the gun and the buncher and just before the section (lens SL used in three gradient method). A schematic diagram of the facility is presented on figure1.

Figure 1: scheme of NEPAL test facility

1 GUN	4 MONITORS	7 SOLENOID	10 SPECTROMETER
2 LENS	5 PRE-BUNCHER	8 ACC. STRUCTURE	11 SLIT
3 STEERING	6 BUNCHER	9 COLLIMATOR	12 BEAM CATCHER
TR TRANSITION RADIATION MONITOR			SL SOLENOIDAL LENS
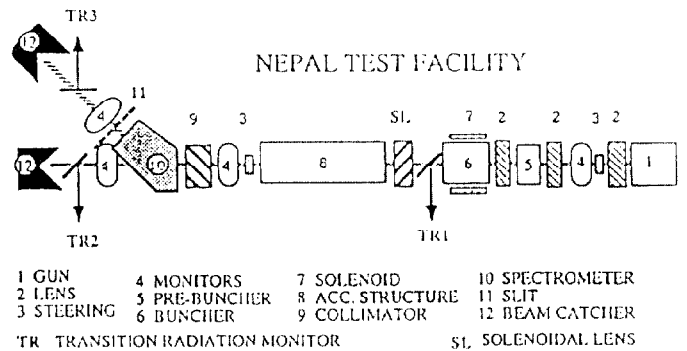
3.2 System configuration

The schematic diagram of the profile monitor is reported on figure 2. The optical image of the beam is transmitted to the CCD camera [RTC 56475] through a telescopic lens system. A very usual transformation ratio f_2/f_1 has been of 2.5. We have also used classical lens with focal length 35 mm. (In the latter case the spatial resolution was of 0.1 mm / element ; optimization of the optics may improve this resolution). The CCD camera has an active

area of 6×4.5 mm^2 with pixels 9.8×9.2 μm^2. Its minimum sensitivity is 10^4 photons/s/pixel. Automatic gain is provided in order to get the best dynamic range for light intensity. The video signal given by the CCD camera is numerized through a DCS01 TEKTRONIX video digitizer. The image - with 256 possible gray levels - is stored in a 512×512 octets memory and analyzed by a dedicated program in C language in a PC computer (COMPAQ). Triggering is ensured with light detection.

Figure 2: Schematic diagram of the profile monitor
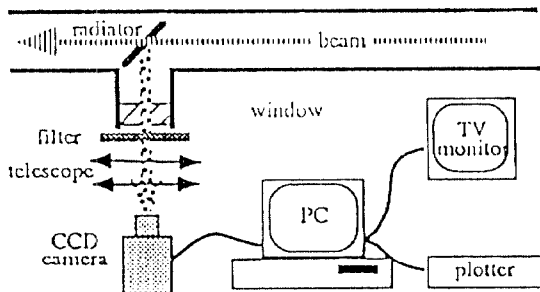
3.3 The program

The program allows unique or averaged acquisitions. The image can be observed on a VGA screen with 16 colours. Many figures could be derived from the digitized data :

- Horizontal or vertical profiles in every chosen point

- Intensity distribution of the beam image

- Pseudo 3D representation (2 dimensional beam distribution)

- Beam width measurements expressed in pixels for a given intensity level.

All images can be stored on floppy disks. As beam images can be displayed for every cycle of linac operation, that system is working as a real-time profile monitor.

4 MEASUREMENTS

Measurements concerned electron beam energies as low as 80 keV to 20 MeV.At 80 keV OTR observations were done using aluminium and silver foils with a thickness of 20 μm. Polarization test, for an electron beam impinging on a silver foil at 30^0 incidence, showed that the main component of polarization vector lied in the incidence plane (formed by the incident ray and the normal to the mirror). The observations at low energy were completed with measurements at energies above 3 MeV. The angular acceptance of the optics (see figure 2) was of 0.35 $Sterad$ quite comparable to the angular aperture of the backward OTR at 3 MeV. The overall OTR photon yield integrated over all angles and in the optical range was above $3\ 10^{-3}$ photon/electron. This value is somewhat lower than the expected one - close to 10^{-2} photon/electron; reflections on the glass window and lenses could explain such lowering. A rough control of the beam position regarding the

accelerator axis is possible by comparison of this position with the cathode image. The latter is then removed by an appropriate filter to do the measurement.

4.1 Emittance measurement

The three gradient method associating an axisymmetric solenoidal lens to the profile monitor is here used. If three profiles are theoretically needed to calculate the three coefficients of the beam emittance ellipse equation, a more larger number - 10 to 20 - is suited and provides precise determination of these coefficients through least square fitting. Using K. Brown formulation [8], the coefficients $\sigma_{ij}(0)$ of the beam matrix in the (0) plane where we wish to know the emittance are related to the transform matrix coefficients R_{ij} from the entrance of the lens to the mirror by the expression:

$$R_{11}^2\sigma_{11}(0) + 2R_{11}R_{12}\sigma_{21}(0) + R_{12}^2\sigma_{22}(0) = \sigma_{11}(1) \quad (2)$$

In that equation, $\sigma_{11}(1)$ represents the square of the measured dimension at the mirror : $\sqrt{\sigma_{11}(1)} = x_m$

5 RESULTS

Measurements have been realized with an electron beam of 100 $nCb/pulse$ with 100 Hz repetition rate.

5.1 Preliminary measurements

Using a moving slit placed before the mirror, we got a set of horizontal profiles when varying the lens magnetic field. Using the three gradient method with appropriate R_{ij} coefficients we derived a beam emittance ϵ of 3π $mm\ mrad$ at $E = 4.8 MeV$ for 90% of the particles. This gives roughly 30 π $mm\ mrad$ as normalized emittance ϵ_n. ($\epsilon_n = \beta\gamma\epsilon$)

5.2 Measurements using OTR

Typical example of beam distributions is shown on figure 3. From this kind of images it is possible to derive the intensity profile in horizontal and vertical plane in terms of intensity versus number of pixels.

Figure 3: Profile distribution

Top: Beam image

Bottom: Beam profile
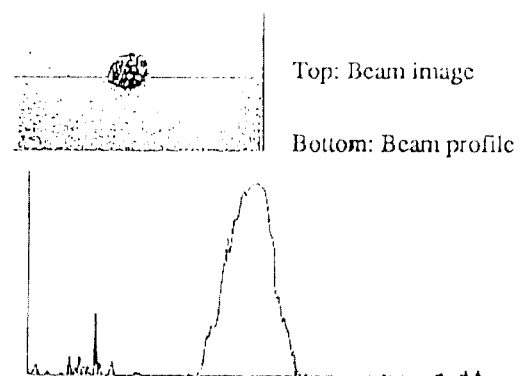
Two-dimensional beam distribution (X-Y) is also available (figure 4). Both representations (X/Y and X-Y) may be observed when changing the lens magnetic field.

Figure 4: Two-Dimensional beam distribution
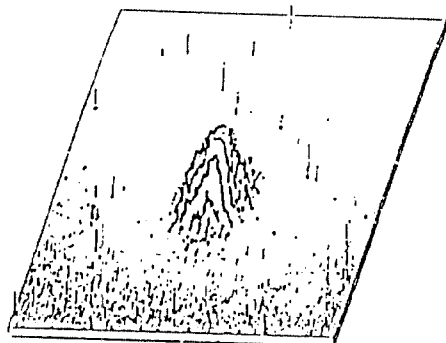
Square beam width variation with lens magnetic field is shown on figure 5. From this data, emittance is determined according to equation (2), using least square fitting.

Figure 5: Square beam width variation
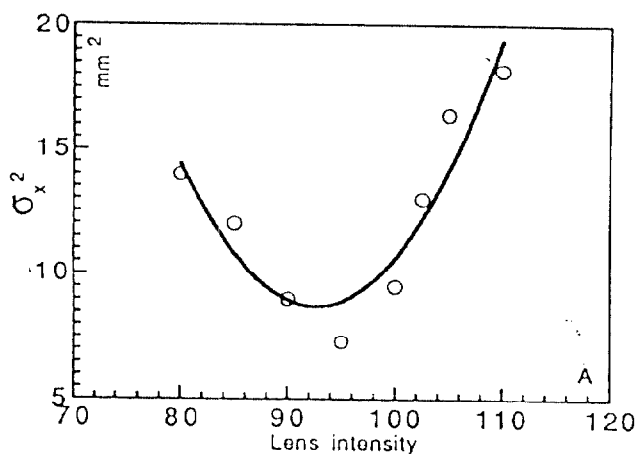
The emittance ellipse for the horizontal plane, at the entrance of the magnetic lens, is represented on figure 6. The numerical value of the emittance - for 90 % of particles - is found to be $4.4 \pi \, mm \, mrad$ at $E = 4.8 \, MeV$. Normalized emittance is therefore $42 \pi \, mm \, mrad$. The discrepancy with the moving slit method - with identical beam conditions and the same amount of particles in the phase space is about 40 %.

A simulation program - PARMELA - [9][10] provided an emittance value for an electron beam of the same intensity (100 $nCb/pulse$ — 100 Hz). A value of 15 $\pi \, mm \, mrad$ as normalized emittance was found. Emittance growth due to second order contributions of optics or disalignememt effects in rf cavities and not considered in simulation may explain such difference with the measurement.

Figure 6: Emittance ellipse
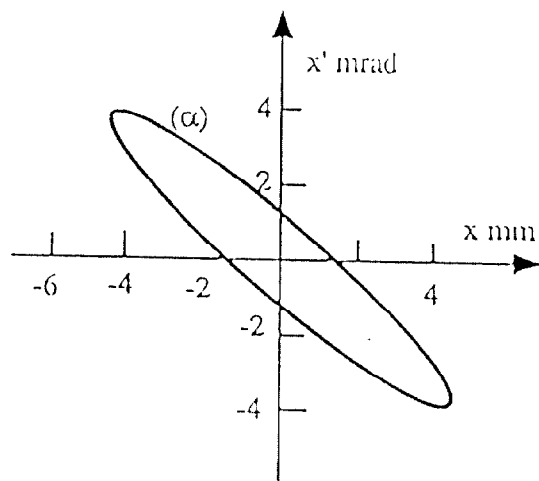
6 SUMMARY AND CONCLUSIONS

The monitor chosen for emittance measurement seems adequate due to its relative sensitivity, its good resolution, the big dynamical range for electron energies, its great rapidity allowing almost real time observation. Improvements could be made and concern mainly the optics between the mirror and the CCD as well as Peltier cooling of the camera which may enhance the signal over noise factor.

7 ACKNOWLEDGEMENTS

8 REFERENCES

[1] V.L. Ginzburg and I.M. Franck JETP 16 (1946) 15

[2] L. Wartski et al. IEEE Trans.Nucl.Sci. 20 (1973) 544

[3] L. Wartski et al. J.Appl.Phys 46 (1975) 3644

[4] D.W. Rule NIM B24/25 (1987) 901

[5] J.C. Ashley Phys.Rev. 155 $n^{0}2$ (1967) 208

[6] A.M. Mahan and A. Gallagher RSI 47 $n^{0}1$ (1976) 81

[7] A. Dubrovin LAL 90-02 Fevrier 1990 Orsay

[8] K.Brown TRANSPORT SLAC-91 May 1977 Stanford

[9] K. Grandall PARMELA: unpublished report

[10] B. Mouton about PARMELA PROGRAM V 4.0 LAL/SERA 90-300 Orsay